NASA/TM—2018–000000

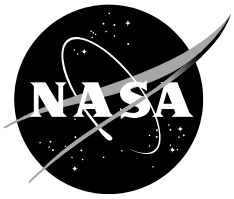

TESS Data Release Notes:
Sector 5, DR7

Michael M. Fausnaugh
Kavli Institute for Astrophysics and Space Science, Massachusetts Institute of Technology, Cambridge, Massachusetts

Christopher J. Burke
Kavli Institute for Astrophysics and Space Science, Massachusetts Institute of Technology, Cambridge, Massachusetts

Douglas A. Caldwell
SETI Institute, Mountain View, California

Jon M. Jenkins
Ames Research Center, Moffett Field, California

Jeffrey C. Smith, Joseph D. Twicken
SETI Institute, Mountain View, California

Roland Vanderspek
Kavli Institute for Astrophysics and Space Science, Massachusetts Institute of Technology, Cambridge, Massachusetts

John P. Doty
Noqsi Aerospace Ltd, Billerica, Massachusetts

Eric B. Ting
Ames Research Center, Moffett Field, California

Joel S. Villasenor
Kavli Institute for Astrophysics and Space Science, Massachusetts Institute of Technology, Cambridge, Massachusetts

January 31, 2019

Acknowledgements

These Data Release Notes provide information on the processing and export of data from the Transiting Exoplanet Survey Satellite (TESS). The data products included in this data release are full frame images (FFIs). Due to a lapse in appropriations, the following data products for this Sector are not available at this time: target pixel files, light curve files, collateral pixel files, cotrending basis vectors (CBVs), and Data Validation (DV) reports, time series, and associated xml files

These data products were generated by the TESS Science Processing Operations Center (SPOC, Jenkins et al., 2016) at NASA Ames Research Center from data collected by the TESS instrument, which is managed by the TESS Payload Operations Center (POC) at Massachusetts Institute of Technology (MIT). The format and content of these data products are documented in the Science Data Product Description Document (SDPDD)[1]. The SPOC science algorithms are based heavily on those of the Kepler Mission science pipeline, and are described in the Kepler Data Processing Handbook (Jenkins, 2017).[2] The Data Validation algorithms are documented in Twicken et al. (2018) and Li et al. (2019). The TESS Instrument Handbook (Vanderspek et al., 2018) contains more information about the TESS instrument design, detector layout, data properties, and mission operations.

The TESS Mission is funded by NASA's Science Mission Directorate.

This report is available in electronic form at
https://archive.stsci.edu/tess/

[1] https://archive.stsci.edu/missions/tess/doc/EXP-TESS-ARC-ICD-TM-0014.pdf
[2] https://archive.stsci.edu/kepler/manuals/KSCI-19081-002-KDPH.pdf

1 Observations

TESS Sector 5 observations include physical orbits 17 and 18 of the spacecraft around the Earth. Data collection was paused for for 1.35 days during perigee passage while downloading data. The use of Camera 1 in attitude control was disabled for the last ~ 0.5 days of Orbit 18 due to strong scattered light signals (see §1.1). In total, there are 25.23 days of science data collected in Sector 5.

Table 1: Sector 5 Observation times

	UTC	TJD[a]	Cadence #
Orbit 17 start	2018-11-15 07:47:48	1437.82566	151467
Orbit 17 end	2018-11-27 16:44:46	1450.19856	160375
Orbit 18 start	2018-11-29 01:09:22	1451.54898	161347
Camera 1 Guiding Disabled	2018-12-11 10:31:39	1463.93945	170269
Orbit 18 end	2018-12-11 21:35:39	1464.40056	170601

[a] TJD = TESS JD = JD - 2,457,000.0

The spacecraft was pointing at RA (J2000): 73.5382°; Dec (J2000): −31.9349°; Roll: 191.05°. Two-minute cadence data were collected for 20,000 targets, and full frame images were collected every 30 minutes. See the TESS project Sector 5 observation page[3] for the coordinates of the spacecraft pointing and center field-of-view of each camera, as well as the detailed target list. Fields-of-view for each camera with all two-minute targets can be found at the TESS Guest Investigator Office observations status page[4].

1.1 Spacecraft Pointing and Momentum dumps

The reaction wheel speeds were reset with momentum dumps every 3.0 days. FFIs taken during these times are marked with bit 6 (Reaction Wheel Desaturation Events) set. Only one or two FFIs are affected by each momentum dump.

At the end of orbit 18, the Earth was $< 35°$ from the boresight of Camera 1. At these low angles, the level of scattered light is too high for meaningful guide star centroids to be measured. Guiding with Camera 1 was therefore disabled at this time, starting at TJD 1463.93945 until the end of the sector. When Camera 1 guiding was disabled, the spacecraft attitude shifted by a small amount, about 1 arc-second (0.05 pixels).

Figure 1 summarizes the pointing performance over the course of the sector based on Fine Pointing telemetry. Disabling Camera 1 guiding near the end of the Sector caused a brief impulse in pointing, which settles out within minutes. The other periods of increased dispersion are generally correlated with the momentum dumps. Several shorter impulse-like events are also evident, which are associated with quasi-instantaneous changes in the internal friction of the reaction wheels.

[3] https://tess.mit.edu/observations/sector-5

[4] https://heasarc.gsfc.nasa.gov/docs/tess/status.html

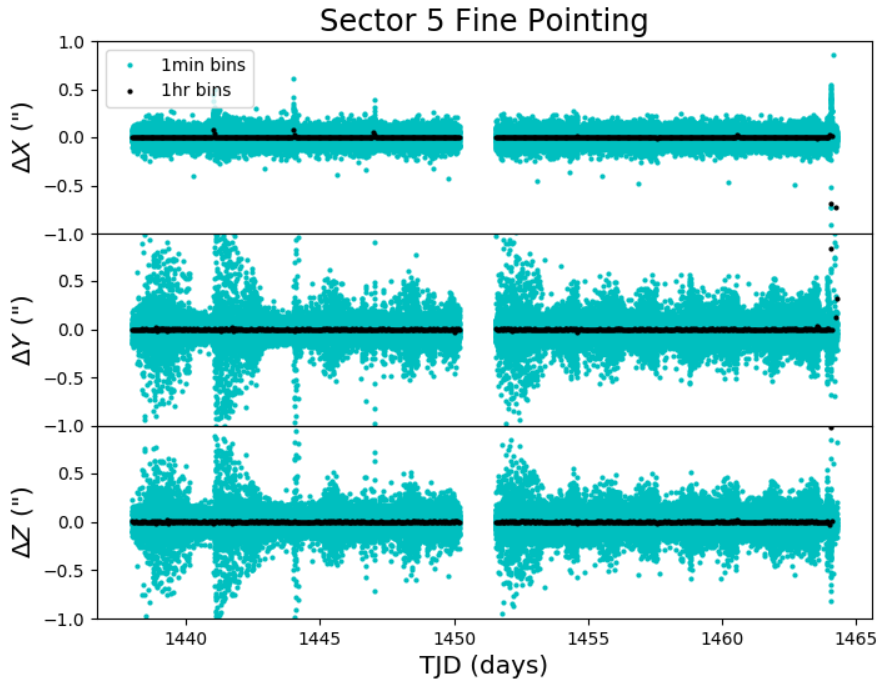

Figure 1: Guiding corrections based on spacecraft fine pointing telemetry. The delta-quaternions from each camera have been converted to spacecraft frame, binned to 1 minute and 1 hour, and averaged across cameras. Long-term trends (such as those caused by differential velocity aberration) have also been removed. The ΔX/ΔY directions represent offsets along the the detectors' rows/columns, while the ΔZ direction represents spacecraft roll. The large dispersion at the end of the sector is caused by disabling Camera 1 for guiding (see §1).

1.2 Scattered Light

Figure 2 shows the angle between each camera's boresight and the Earth or Moon—this figure can be used to identify periods affected by scattered light and the relative contributions of the Earth and Moon to the image backgrounds.

2 Anomalous Effects

2.1 Smear Correction Issues

In Sector 5, we have not found any problematic smear corrections, beyond the known charge traps that affect the smear correction estimate. We have identified some moderately bright stars in the upper buffer rows that affect the first row of the virtual smear region. However, the smear correction is robust against these cases.

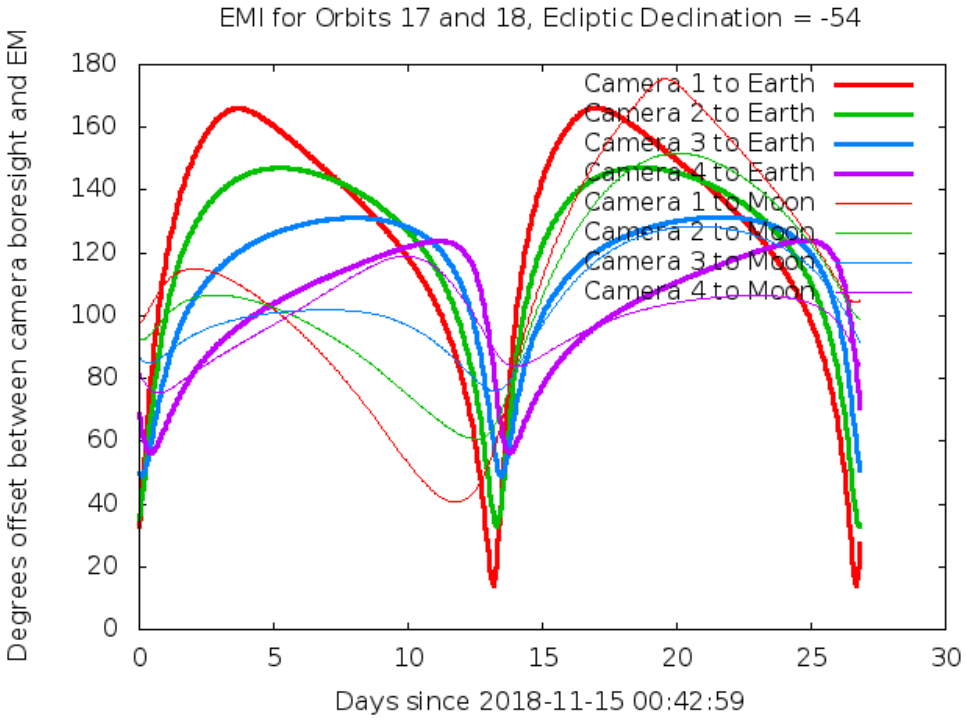

Figure 2: Angle between the four camera boresights and the Earth/Moon as a function of time. When the Earth/Moon moves within 37° of a camera's boresight, scattered light patterns and complicated features such as glints may appear. At larger angles, low level patchy features may appear. This figure can be used to identify periods affected by scattered light and the relative contributions of the Earth and Moon to the background. However, the background intensity and locations of scattered light features depend on additional factors, such as the Earth/Moon azimuth and distance from the spacecraft.

2.2 Fireflies and Fireworks

Table 2 lists all firefly and fireworks events for Sector 5. These phenomena are small, spatially extended, comet-like features in the images that may appear one or two at a time (fireflies) or in large groups (fireworks). See the Instrument Handbook for a complete description.

2.3 TJD Calculation

The spacecraft clock drifts slowly relative to UTC time at a rate of ∼35 milliseconds per day. This drift is captured in a clock kernel that is used to calculate TJD from spacecraft time. The calculated clock kernel correcting this difference is based on the measured drift rate from periodic S-band and Ka-band ranging contacts.

The clock kernel used to calculate TJD in Sector 5 used ranging data collected only through late August, 2018; as a result, the extrapolation to Sector 5 times is slightly off. The error between true and calculated times grew linearly with time since August 2018, so that the calculated TJD values in all data products are offset from the correct values by ∼1.7 seconds at the end of orbit 18 (2018-12-11 UTC). This difference also implies that the durations of

Table 2: Sector Fireflies and Fireworks

FFI Start	FFI End	Cameras	Description
2018319172939	2018319182939	1, 2, 3	Fireflies
2018321095939	2018321102939	2, 3, 4	Fireflies
2018324152939	2018324155939	2, 4	Fireflies
2018325082939	2018325085939	3, 4	Firefly
2018327185939	2018327192939	1, 2, 3	Fireflies
2018328092939	2018328095939	1, 2, 3	Firefly
2018333052939	2018333055939	1	Firefly
2018335185939	2018335192939	1, 2, 3, 4	Fireworks
2018336125939	2018336132939	3	Firefly
2018338085939	2018338092939	2	Firefly
2018338185939	2018338192939	3	Firefly
2018339002939	2018339005939	4	Firefly

the FFIs, as calculated by the difference between the TSTOP and TSTART times, is low by about 280 microseconds. This issue will be corrected if the data are reprocessed in a future data release.

References

Jenkins, J. M. 2017, Kepler Data Processing Handbook: Overview of the Science Operations Center, Tech. rep., NASA Ames Research Center

Jenkins, J. M., Twicken, J. D., McCauliff, S., et al. 2016, in Proc. SPIE, Vol. 9913, Software and Cyberinfrastructure for Astronomy IV, 99133E

Li, J., Tenenbaum, P., Twicken, J. D., et al. 2019, *PASP*, 131, 024506

Twicken, J. D., Catanzarite, J. H., Clarke, B. D., et al. 2018, *PASP*, 130, 064502

Vanderspek, R., Doty, J., Fausnaugh, M., et al. 2018, TESS Instrument Handbook, Tech. rep., Kavli Institute for Astrophysics and Space Science, Massachusetts Institute of Technology

Acronyms and Abbreviation List

BTJD Barycentric-corrected TESS Julian Date

CAL Calibration Pipeline Module

CBV Cotrending Basis Vector

CCD Charge Coupled Device

CDPP Combined Differential Photometric Precision

COA Compute Optimal Aperture Pipeline Module

CSCI Computer Software Configuration Item

CTE Charge Transfer Efficiency

Dec Declination

DR Data Release

DV Data Validation Pipeline Module

DVA Differential Velocity Aberration

FFI Full Frame Image

FIN FFI Index Number

FITS Flexible Image Transport System

FOV Field of View

FPG Focal Plane Geometry model

KDPH Kepler Data Processing Handbook

KIH Kepler Instrument Handbook

KOI Kepler Object of Interest

MAD Median Absolute Deviation

MAP Maximum A Posteriori

MAST Mikulski Archive for Space Telescopes

MES Multiple Event Statistic

NAS NASA Advanced Supercomputing Division

PA Photometric Analysis Pipeline Module

PDC Pre-Search Data Conditioning Pipeline Module

PDC-MAP Pre-Search Data Conditioning Maximum A Posteriori algorithm

PDC-msMAP Pre-Search Data Conditioning Multiscale Maximum A Posteriori algorithm

PDF Portable Document Format

POC Payload Operations Center

POU Propagation of Uncertainties

ppm Parts-per-million

PRF Pixel Response Function

RA Right Ascension

RMS Root Mean Square

SAP Simple Aperture Photometry

SDPDD Science Data Product Description Document

SNR Signal-to-Noise Ratio

SPOC Science Processing Operations Center

SVD Singular Value Decomposition

TCE Threshold Crossing Event

TESS Transiting Exoplanet Survey Satellite

TIC TESS Input Catalog

TIH TESS Instrument Handbook

TJD TESS Julian Date

TOI TESS Object of Interest

TPS Transiting Planet Search Pipeline Module

UTC Coordinated Universal Time

XML Extensible Markup Language